EARTHQUAKE-INDUCED PRESSURES ON A RIGID WALL STRUCTURE

J. H. Wood*

SUMMARY

This paper describes the application of linear elastic theory to estimate the earthquake-induced soil pressures on a wall forming part of the structure of a power station founded on rock.

Analyses showed that the Mononobe-Okabe assumptions would not be applicable for this relatively rigid wall structure and it was found that elasticity theory gave greater forces and moments than would be obtained by using the Mononobe-Okabe method. The extent to which deformations of the structure and its foundations influence the wall pressures was investigated. It was found that even for this relatively rigid structure and foundation, the displacements resulting from the inertia of the wall structure can produce a significant increase in the total forces acting on the wall.

1. INTRODUCTION

The behaviour of wall structures during earthquakes can be broadly classified into three categories defined by the maximum stress condition that develops in the soil near the wall. The soil may remain essentially elastic, respond in a significantly nonlinear manner or become fully plastic. The rigidity of the wall and its foundations will have a strong influence on the type of soil stress condition that develops. It is well known that flexible structures, such as cantilever walls, displace sufficiently under the action of gravity forces alone to produce a fully plastic stress condition in most soils. For rigid walls on rock or pile foundations the soil stresses may remain essentially elastic under combined gravity and earthquake forces. The pressures on basement walls in buildings are often influenced by the dynamic properties of the building since the inertia forces acting on the structure may produce significant displacements of the wall relative to the surrounding soil. Even relatively small wall displacements can produce appreciable changes to the soil pressures acting on the wall.

An essentially exact formulation of the interaction of wall structures and the supported soil during earthquakes yields a highly intractable problem governed by three-dimensional wave equations for a nonlinear inhomogenous medium. Exact solutions are not possible and even if numerical methods such as the finite element method are used it is necessary to make simplifying assumptions. The development of more sophisticated computer programmes will enable more exact analyses to be attempted; however, the degree of accuracy obtainable is limited because the basic input parameters cannot be precisely specified. Many soil-retaining structures will not be of sufficient importance to warrant more than a very basic soil investigation and only in exceptional circumstances would a soil investigation be sufficiently detailed to enable a good prediction of the soil behaviour under dynamic loading. Uncertainty exists regarding the magnitude and frequency composition of incoming earthquake waves at any particular site. At the present time the nature of the mechanism generating the waves is not precisely known and no satisfactory method exists for predicting the modifying effects of the geology along the travel paths. Even if generation and modification of the earthquake waves could be accurately modelled, uncertainty would exist regarding the relative location of possible epicentres for major earthquakes. In view of the limitations in the basic input parameters, the estimation of earthquake-induced pressures by approximate methods can be frequently justified. However, it is important to account for wall displacements and use a method appropriate for the stress condition that developes in the soil.

The most generally accepted approach for estimating earthquake-induced pressures is the Mononobe-Okabe method [3,4,5] which is based on an approximate plasticity theory and is essentially an extension of the well known Coulomb method for static pressures. It is assumed that the wall deformations are sufficiently large to induce a fully plastic stress condition in the soil near the wall. This assumption is unlikely to be satisfied for building basement walls or other rigid wall structures founded on firm soil or rock and for these cases a method based on elasticity theory is likely to be more appropriate.

This paper describes the application of a number of approximate elasticity methods to compute earthquake-induced pressures on a soil-retaining wall in the Castaic power station, California. The

* Structures Engineer, Central Laboratories, Ministry of Works and Development.

Mononobe-Okabe assumptions were not satisfied for this example and comparisons made between the Mononobe-Okabe and elasticity results indicated that the Mononobe-Okabe approach would underestimate the total force and moment on the wall. In applying elasticity theory to the power station wall it was necessary to make a number of simplifying assumptions regarding the input earthquake motion, the soil behaviour and the deformations of the structure and its foundations. In particular, it was assumed that the earthquake ground shaking could be represented by a known horizontal acceleration function acting at the rock foundation level. For convenience the acceleration function was represented by a smoothed acceleration response spectrum.

2. CASTAIC POWER STATION

The Castaic power station was designed and constructed as a joint venture by the City of Los Angeles and the California State Department of Water Resources. The plant is a 1,250,000 kilowatt reversible-turbine hydro-electric facility located approximately 70 km northwest of downtown Los Angeles and about 18 km from the San Andreas fault. A typical cross-section of the powerhouse, which shows the extent of the soil retaining function of one face of the structure, is shown in Fig. 1. Details of the structure are shown in Fig. 2.

Preliminary studies showed that because of the rock foundation and the rigid nature of the wall structure, a relatively good approximation for earthquake-induced pressures could be obtained by assuming rigid wall behaviour. In the following sections solutions are obtained for both perfectly rigid-wall behaviour and for the case where the structure was permitted to undergo elastic rotation on its foundation.

3. RIGID WALL ANALYSIS

Earthquake induced wall pressures were computed for the rigid wall case using a static finite element method, a normal mode dynamic finite element method and an analytical normal mode solution for a related problem.

The finite element mesh used for the dynamic analysis is shown in Fig 3. A finer mesh with 1.52 m by 1.52 m elements in the vicinity of the wall was used for the static solutions. The finite element analyses were undertaken for both assumptions of smooth and fully bonded contact between the wall and soil. The other boundary conditions assumed are shown in Fig 3.

Details of static and normal mode analytical solutions for a related problem are given by Wood [5]. These solutions are for the case of a simple rectangular boundary configuration with smooth contact between the elastic soil and the wall boundary. The geometry and boundary conditions of the related problem are shown in Fig 4.

Soil properties were obtained by triaxial testing of the backfill material and the following average values were adopted for the analyses;

Youngs Modulus	E	=	48 MPa
Poisson's Ratio	ν	=	0.4
Unit weight	γ	=	1920 kg/m^3

The analytical solution was evaluated assuming that the prototype problem could be represented by an approximate equivalent rectangle of soil having a geometric ratio $\frac{L}{H} = 1.67$.

The static pressure distributions for a one-g horizontal body force and the significant modal pressure contributions obtained from the dynamic analyses are plotted in Fig 5. The modal pressure distributions have been normalised so that the aljebraic summation of all the modal contributions gives the static solution for a horizontal one-g body force. The modal contributions normalised in this manner are referred to as the static-one-g modal pressure distributions. It should be noted that the maximum earthquake induced modal pressures can be readily obtained by scaling the static-one-g contributions by response factors from the earthquake acceleration spectrum. Gravity induced pressures are not included in the plotted results.

The natural frequencies of the modes that gave significant contribution to the wall pressure distributions are given in Table 1.

Maximum earthquake-induced pressure distributions were computed using the Response Spectrum method, and Housner's 10% damped velocity spectrum given in References 1 and 5. The effects of the higher modes were included by using a "rigid" mode having a pressure distribution the difference between the appropriate static solution and the sum of the two modal contributions for the bonded wall and the three contributions for both the smooth wall solutions. This "rigid" mode distribution was assumed to contribute at an acceleration of 0.33 g (that is the peak ground acceleration). Plots of the pressure distributions obtained by taking the root-mean-square sums and the algebraic sums of the modal contributions (including the "rigid" mode) are given in Fig. 6. The large difference between the rms and the algebraic sums of the modal pressures for the smooth wall cases is due to the relatively similar magnitude of two of the modal contributions. In the bonded contact case most of the pressure response comes from a single mode and thus the difference between the pressures summed by the two methods is relatively small. Previous studies showed that near $\frac{L}{H}$ values of 2.0 the relative magnitude of the modal pressure contributions of the analytical solution were quite sensitive to the value of the $\frac{L}{H}$ parameter. Better agreement between the bonded and the smooth contact solutions would be expected for values of equivalent $\frac{L}{H}$ greater than 2.5 and for equivalent $\frac{L}{H}$ values between 0.5 and 1.5. In these ranges the relative participation of the modal contributions becomes less sensitive to changes in the geometry and boundary conditions.

For cases in which a significant difference occurs between the rms and

algebraic sum it would appear reasonable to use for design a pressure distribution intermediate between the two results or to at least consider the consequence of an unfavourable combination of the modes.

If it is assumed that the soil satisfies the Mohr-Coulomb failure criterion then the horizontal stress required to produce failure in the soil is approximately

$$\frac{\sigma_{x\ max}}{\gamma\ H} = Kp\ (1 - \frac{y}{H}) \qquad (1)$$

in which Kp = passive earth-pressure coefficient. By combining the gravity horizontal pressures on the wall with the maximum earthquake pressures given in Fig. 6 it is apparent that soil failure is only likely for $\frac{y}{H}$ greater than 0.9. Consequently the assumption of linear elastic behaviour of the soil appears satisfactory for this example.

Forces and moments on the wall were computed for the smooth contact analytical solutions by integration of the pressure distributions given in Fig. 5. These values are compared in Table 2 with forces and moments computed by the Mononobe-Okabe method and with forces and moments computed for vertical gravity effects. To compute the Mononobe-Okabe values the usual assumption of a triangular pressure distribution with maximum pressure at the base of the wall was made. The angle of internal friction of the soil was taken as 35° and zero vertical acceleration assumed. For these assumptions Seed and Whitman [4] give the following approximate relationship for the earthquake force increment on the wall.

$$\frac{\Delta P_{AE}}{\gamma H^2} = \frac{3}{8} k_h \qquad (2)$$

in which

ΔP_{AE} = active wall force increment due to horizontal earthquake load

k_h = horizontal earthquake coefficient

The forces and moments from the Mononobe-Okabe method are lower than the values obtained by the other methods. Because of the rigid nature of the wall and foundation, and because the soil is expected to remain essentially elastic the Mononobe-Okabe method is not suitable for this problem. The discrepancy between the Mononobe-Okabe method and the elasticity solutions will increase for values of $\frac{L}{H}$ greater than 1.67. This is illustrated in Fig 7 by plots of forces and moments obtained from a static theory of elasticy solution. The results show that forces on a rigid wall can be expected to increase with increasing $\frac{L}{H}$ and that this increase is significant for $\frac{L}{H}$ up to 5.

The results given in Table 2 indicate that the earthquake forces and moments from the static theory of elasticity solution tend to be conservative and so this approach can be used to give a satisfactory first approximation for many problems. It can also be seen that the earthquake forces and moments are of the same order of magnitude as gravity effects.

4. ROTATING WALL ANALYSIS

A preliminary study indicated that the small horizontal displacements of the powerhouse structure under earthquake loads would result mainly from the rigid body rotation of the structure on its rock foundation. In order to derive an analytical solution for the dynamic behaviour including the effects of wall rotation the idealized problem shown in Fig 8 was studied. The foundation rotational stiffness per unit length is represented by a spring of stiffness k_w and the dissipation associated with the rotational deformation of the foundation is represented by a dashpot with damping coefficient c_w. By replacing the boundary forcing by d'Alembert body forcing the displacement equations of motion of the elastic soil can be written in vector form as

$$L\underline{u}(x,y,t) = \rho\ddot{\underline{u}}(x,y,t) + c\dot{\underline{u}}(x,y,t) + \rho\ddot{\underline{u}}_b(t) \qquad (3)$$

in which

L = linear operator with respect to the spatial co-ordinates

$\underline{u}(x,y,t) = \begin{Bmatrix} u(x,y,t) \\ v(x,y,t) \end{Bmatrix}$, vector of the displacement components u and v

$\underline{u}_b(t) = \begin{Bmatrix} u_b(t) \\ 0 \end{Bmatrix}$, vector of displacements on the rigid boundary

c = damping coefficient

ρ = mass density of soil

By superposition it is readily shown that the general solution of equation (3) can be expressed as

$$\underline{u}(x,y,t) = \underline{u}_r(x,y,t) + \underline{u}_f(x,y,t) \qquad (4)$$

in which

$\underline{u}_r(x,y,t)$ = rigid-wall solution; that is, solution for $u(0,y,t) = 0$

$\underline{u}_f(x,y,t)$ = forced-wall solution; that is, solution of equation (3) with $\underline{u}_b(t) = \underline{0}$, for forcing of the wall boundary by the horizontal wall displacement $u(0,y,t)$ from the general solution of equation (3)

The equation of motion for the wall structure may be written as

$$I_w\ddot{\theta}(t) + c_wH^2\dot{\theta}(t) + k_wH^2\theta(t) + m_wh_c\ddot{u}_b(t) - M_r(t) - M_f(t) = 0 \qquad (5)$$

in which

I_w = moment of inertia of wall about the base

m_w = mass of wall structure

h_c = height of center of gravity of wall structure above the base

$$M_r(t) = \int_o^H y\left[L_p \underline{u}_r\ (x,y,t)\right]_{x=0} dy, \text{dynamic moment on rigid wall}$$

$$M_f(t) = \int_o^H y\left[L_p \underline{u}_f(x,y,t)\right]_{x=0} dy, \text{ moment on dynamically forced wall}$$

L_p = linear operator defined by

$$\sigma_x(x,y,t) = L_p\ \underline{u}(x,y,t)$$

σ_x = stress in x direction

A unit length of structure is implied for the constants in expression (5) and for M_r and M_f. The moments are assumed to be positive when acting in the clockwise direction.

Let the Fourier transform of the function $\ddot{u}_b(t)$ be defined as

$$\bar{\ddot{u}}_b(\omega) = \int_{-\infty}^{\infty} \ddot{u}_b(t) e^{-i\omega t}\, dt \qquad (6)$$

Using this definition the Fourier transformation of equation (5) can be written as

$$\left[-\omega^2 I_w + i\omega c_w H^2 + k_w H^2\right]\bar{\theta}(\omega) + \bar{\ddot{u}}_b(\omega) m_w h_c - \bar{M}_r(\omega) - \bar{M}_f(\omega) = 0 \qquad (7)$$

(A bar over the symbol is used to denote a transformed variable.) The transformed moments can be expressed as

$$\bar{M}_r(\omega) = \bar{M}_r'(\omega)\ \frac{\bar{\ddot{u}}_b(\omega)}{g}$$

$$\bar{M}_f(\omega) = \bar{M}_f'(\omega)\bar{\theta}(\omega) \qquad (8)$$

in which

$\bar{M}_r'(\omega)$ = complex-amplitude of steady-state moment on rigid-wall for one-g amplitude base forcing

$\bar{M}_f'(\omega)$ = complex-amplitude of steady-state moment for harmonic wall-forcing of unit rotational amplitude

Let

$$\omega_w = \sqrt{\frac{k_w H^2}{I_w}} \qquad (9)$$

$$\zeta_w = \frac{c_w H^2}{2\omega_w I_w}$$

Rearrangement of equation (7) and substitution of equations (8) and (9) gives

$$\bar{\theta}(\omega) = \frac{-\left[m_w g h_c - \bar{M}_r'(\omega)\right]\bar{\ddot{u}}_b(\omega)}{g\omega_w^2 I_w\left[1 - \frac{\omega^2}{\omega_w^2} + 2i\zeta_w\frac{\omega}{\omega_w} - \frac{\bar{M}_f'(\omega)}{\omega_w^2 I_w}\right]} \qquad (10)$$

The transformed total wall moment $\bar{M}_T(\omega)$ can be expressed as

$$\frac{\bar{M}_T(\omega)}{M_{sr}} = \frac{M_{sf}}{M_{sr}}\frac{\bar{M}_f'(\omega)\bar{\theta}(\omega)}{M_{sf}} + \frac{\bar{M}_r'(\omega)}{M_{sr}}\frac{\bar{\ddot{u}}_g(\omega)}{g} \qquad (11)$$

in which

M_{sf} = moment on statically forced wall for unit rotation

M_{sr} = moment on rigid-wall from one-g static horizontal body force

Let

$$\frac{\bar{M}_r'(\omega)}{M_{sr}} = r_1(\omega) + ir_2(\omega) \qquad (12)$$

$$\frac{\bar{M}_f'(\omega)}{M_{sf}} = f_1(\omega) + if_2(\omega)$$

The functions $r_1(w)$ and $r_2(w)$ are the real and imaginary parts of the complex-amplitude of moment ratio for harmonic base forcing of a rigid-wall. The functions $f_1(w)$ and $f_2(w)$ are the real and imaginary parts of the complex-amplitude of moment ratio for a harmonically-forced rotating wall. These functions have been evaluated by Wood [5] for a range of the significant parameters.

Substitution of expressions (10) and (12) into (11) gives

$$\frac{\bar{M}_T(\omega)}{M_{sr}} = -\left[\frac{M_s^r(f_1 + if_2)\left\{1 - M_{sr}^d(r_1 + ir_2)\right\}}{\left(1 - \frac{\omega^2}{\omega_w^2}\right) + 2i\zeta_w\frac{\omega}{\omega_w} - M_{sf}^d(f_1 + if_2)} - (r_1 + ir_2)\right]\frac{\bar{\ddot{u}}_b(\omega)}{g} \qquad (13)$$

in which

$$M_{sf}^d = \frac{M_{sf}}{\omega_w^2 I_w}$$

$$M_{sr}^d = \frac{M_{sr}}{m_w g h_c}$$

$$M_s^r = \frac{M_{sf}^d}{M_{sr}^d}$$

Separating the numerator and denominator of expression (13) into real and imaginary parts gives

$$\frac{\bar{M}_T(\omega)}{M_{sr}} = -\frac{\left[f_1 M_s^r - r_1\left(1 - \frac{\omega^2}{\omega_w^2}\right) + 2r_2\zeta_w\frac{\omega}{\omega_w}\right] + i\left[f_2 M_s^r - r_2\left(1 - \frac{\omega^2}{\omega^2}\right) - 2r_1\zeta_w\frac{\omega}{\omega_w}\right]}{\left(1 - \frac{\omega^2}{\omega_w^2} - M_{sf}^d f_1\right) + i\left(2\zeta_w\frac{\omega}{\omega_w} - M_{sf}^d f_2\right)} \times \frac{\bar{\ddot{u}}_b(\omega)}{g} \qquad (14)$$

Or

$$\bar{M}_T(\omega) = \bar{M}'_T(\omega)\,\frac{\bar{\ddot{u}}_b(\omega)}{g} \qquad (15)$$

The time history of the total wall moment can be computed by taking the inverse transform of expression (15). That is

$$M_T(t) = \frac{1}{2\pi}\int_{-\infty}^{\infty} \bar{M}'_T(\omega)\,\frac{\bar{\ddot{u}}_b(\omega)}{g}\,e^{i\omega t}\,d\omega \qquad (16)$$

Thus to evaluate $M_T(t)$ it is necessary to compute the Fourier transform of the base acceleration and to compute the inverse transform of the product specified in expression (16). The Fourier transformation and the inverse transformation can be readily evaluated using a Fast Fourier Transform computer programme.

Frequently an estimate of the maximum earthquake-induced wall moment or pressure distribution is sufficient information for design purposes. Estimates of the maximum forces and pressures can be obtained using random vibration theory and this approach requires considerably less computation than evaluation of complete time-histories using the Fourier transform method. From random vibration theory the variance of the total wall moment can be expressed as

$$s_M^2 = \int_0^{\infty} |\bar{M}'_T(\omega)|^2 G(\omega)\,d\omega \qquad (17)$$

in which

s_M^2 = variance of the total wall moment

$G(\omega)$ = power spectral density of earthquake acceleration (assumed to be random Gaussian process with Zero mean).

$|\bar{M}'_T(\omega)|$ is defined by expressions (14) and (15)

A statistical estimate of the maximum value of the wall moment can be found from the value of s_M^2 and the properties of the normal distribution.

Estimates of the power station dynamic parameters and foundation moduli were made from the design data. The steady-state complex-amplitude response function for total moment given in expression (14) was evaluated using the following values;

natural angular frequency of structure (rigid body rotation)

ω_w = 25.1 rad/s

damping, ζ_w = 5.0%

weight of structure, m_w = 2.2×10^6 kg/m

height of center of gravity above base, h_c = 18.3 m

moment of inertia about base, $I_w = m_w \times (660\ m^2)$

length of structure = 128 m

The functions $r_1(w)$, $r_2(w)$, $f_1(w)$ and $f_2(w)$ were taken from the results given by Wood [5] for the case of $\frac{L}{H}$ = 2.0 and ν = 0.4. The solution obtained for the modulus of the complex-amplitude of total moment is compared in Fig. 9 with the modulus of the complex-amplitude of the rigid-wall moment. The dimensionless frequency used in the plot is the forcing frequency divided by the frequency of the lowest pure shear mode of an infinite elastic stratum with the same depth and elastic moduli as the soil behind the wall. Rotation of the structure reduces the rigid-wall moment in the dimensionless frequency 0 to 1.25. At dimensionless frequencies between 1.25 and 5.5 the total moment is greater than the rigid-wall moment and the maximum difference between the moments occurs close to the natural frequency of the structure (Ω = 4.9).

The variance of the total wall moments was evaluated using expression (17) and an earthquake power spectral density function approximately equivalent to Housner's 10% damped velocity spectra (see References 2 and 5). From the properties of the normal distribution a value of 2.5 times s_M will not be exceeded in an earthquake at a probability of 0.988. The P = 0.988 wall moments were computed to be

Rigid Structure $M_T/\gamma H^3$ = 0.076

Rotating Structure $M_T/\gamma H^3$ = 0.083

Thus the maximum earthquake induced wall moment is greater for the rotating structure case by about 9%.

5. ROTATING WALL APPROXIMATE ANALYSIS

Approximate dynamic soil pressures may be estimated by decomposing the problem into two idealized uncoupled dynamic problems and superimposing the maximum pressures computed for each case by taking an rms sum. The decomposition into the two separate problems is shown diagramatically in Fig. 10. In applying this approximation it is assumed that only weak dynamic coupling exists between the wall structure and the soil body. This will be the case when the lowest natural frequencies of the soil body differ significantly from the lowest natural frequencies of the structure.

Problem I. Only the d'Alembert body forcing of the soil layer is considered in this part of the solution. If the structure is relatively rigid an acceptable Problem I solution can be derived from rigid-wall dynamic

solutions. An improvement to the rigid-wall solution can be made by computing the deflection of the structure under the maximum rigid-wall dynamic pressure and adjusting the solution in accordance with this deflection.

Problem II. Only the d'Alembert forcing on the structure is considered in this part of the solution. A good approximation for the wall pressures can be obtained in many cases by considering the participation of the first mode of vibration of the structure. If the first mode shape is approximately linear the solutions given by Wood [5] for harmonically forced rotating walls may be applied to give a direct solution. The solution for the moment on a harmonically forced rotating wall bounding an elastic soil layer with geometric parameter $\frac{L}{H}$ = 20.0 is shown in Fig 11. (This solution is satisfactory for all $\frac{L}{H}$ values greater than 10). The moment components plotted have been made dimensionless by dividing by the static moment. The forcing frequency has been converted to dimensionless form by dividing by the frequency of the fundamental pure shear mode of an infinite stratum of the same depth and with the same elastic moduli as the elastic soil body.

In most cases the fundamental frequency of the structure will not be significantly modified by the restraint imposed by the soil in contact with the walls.

The three lowest dimensionless natural frequencies of the soil body in the example under discussion ($\frac{L}{H}$ = 2.0, ν= 0.4) are 1.85, 2.41 and 3.94 and compare with a value of 4.91 for the rigid body rotation of the structure. Thus, significant coupling between the structure and the soil body is unlikely and the approximate method is suitable.

A satisfactory Probelm I moment M_I for the present example can be evaluated using the rigid wall assumption. The rigid-wall moment computed using the Response Spectrum method and the rms sum of the modal contributions can be expressed in dimensionless form as $M_I / \gamma H^3 = 0.071$. The maximum rotational response of the structure was computed using Housner's 5% damped relative-velocity spectrum. From this rotation and the harmonically forced rotating wall solutions the Problem II dimensionless moment was evaluated to be $M_{II} / \gamma H^3 = 0.031$. Using the rms sum of M_I and M_{II} a total maximum wall moment of $M_T / \gamma H^3 = 0.078$ was obtained; that is, a 10% increase in the rigid-wall moment.

6. CONCLUSIONS

(1) Because of the complexity of the dynamic interaction of wall structures during earthquakes and the lack of precision with which the basic input parameters are known, exact solutions for earthquake-induced pressures cannot be obtained. Approximate analyses may yield satisfactory solutions for design provided that the simplifying assumptions are appropriate.

(2) The Mononobe-Okabe method will give satisfactory approximate solutions for many wall structures. However, the basic assumption of sufficient wall displacement to produce a fully plastic stress condition in the soil must be satisfied. The method is suitable for relatively flexible walls and cases where the structure can displace along failure planes in the surrounding soil.

(3) The Mononobe-Okabe method may not be suitable for rigid walls on rock or pile foundations and for basement walls in building structures. Approximate solutions for many rigid wall problems can be obtained by using the theory of elasticity.

(4) Displacements resulting from inertia forces acting on the structure should be considered. Relatively small displacements can produce significant modification to the pressure distribution. Influences produced by inertia forces on the structure can be readily considered in elasticity methods.

(5) Static analyses using elasticity theory will give reasonable approximations for earthquake pressures on relatively rigid low walls that do not have appreciable mass.

(6) A satisfactory estimate of the maximum earthquake-induced pressures and forces on basement walls in buildings on relatively rigid foundations can often be made by taking an rms sum of values computed for the assumption of perfectly rigid wall behaviour and values from a forced-wall solution evaluated for the response of the first mode of vibration of the structure.

ACKNOWLEDGEMENTS

The work reported in this paper was undertaken at California Institute of Technology during the author's study leave from the New Zealand Ministry of Works and Development. The author wishes to thank Professor George W. Housner for his guidance with this research.

The financial support received during the author's study leave is gratefully acknowledged. Assistance was received from, the Ministry of Works and Development, California Institute of Technology, U.S. Educational Foundation, U.S. National Science Foundation and the Earthquake Research Affiliates Program at Caltech.

REFERENCES

1. Housner, G. W., Response Spectra Prepared for, "Nuclear Reactors and Earthquakes," Report No. TID 7024, U.S. Atomic Energy Commission, August, 1963.
2. Housner, G. W. and Jennings, P. C., "Generation of Artificial Earthquakes", Journal of the Engineering Mechanics Division, ASCE, Vol. 90, No. EM1, January, 1964.
3. Mononobe, N. and Matsuo, M., "On the Determination of Earth Pressures During Earthquakes," Proceedings, World Engineering Congress, Vol. 9, 1929.
4. Seed, H. B. and Whitman, R. V., "Design of Earth Retaining Structures for Dynamic Loads," ASCE, Specialty Conference, Lateral Stresses in the Ground and the Design of Earth-Retaining Structures, Cornell University, 1970.

5. Wood, J. H., "Earthquake-Induced Soil Pressures on Structures", Report No. EERL 73-05, Earthquake Engineering Research Laboratory, California Institute of Technology, Pasadena, 1973.

TABLE 1.

NATURAL FREQUENCIES

F.E.Bonded		F.E. Smooth		Analytical	
Mode*	Freq. Hz	Mode*	Freq. Hz	Mode	Freq. Hz
1	1.82	1	1.68	1,1	1.58
6	3.68	2	2.00	1,2	2.14
		7	3.85	1,3	3.42

* Mode number in order of increasing frequency as given by the finite element analyses.

TABLE 2.

FORCES AND MOMENTS

Rigid wall Smooth Contact, $\frac{L}{H} = 1.67$, $\nu = 0.4$

Method of Computation	Force/ γH^2	Moment/ γH^3
Response Spectrum, 10% damping, rms sum	0.136	0.076
Response Spectrum 10% damping, absolute sum	0.231	0.122
Static Solution for $k_h = 0.33$ g (elastic, analytical)	0.215	0.116
Mononobe-Okabe for $k_h = 0.33$ g (triangular pressure distribution)	0.124	0.041
Vertical Gravity (elastic, analytical)	0.333	0.111

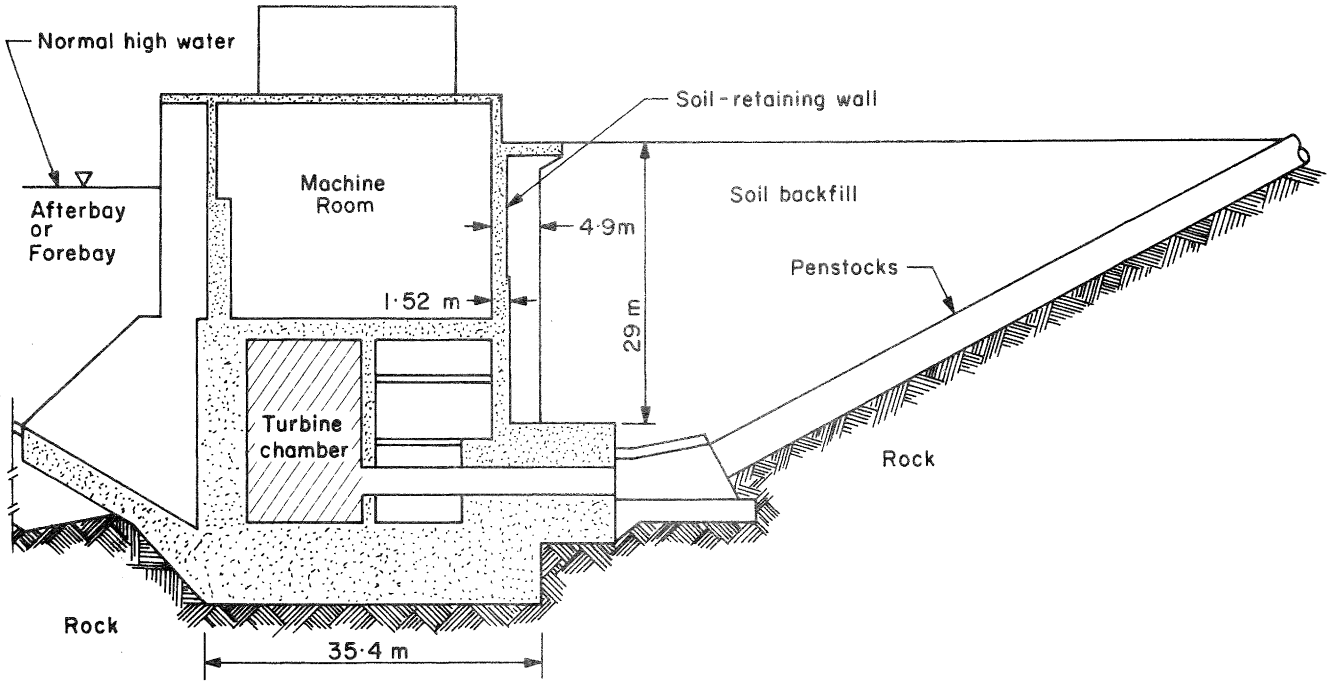

FIGURE 1: CASTAIC POWER STATION. TYPICAL CROSS-SECTION.

FIGURE 2: CASTAIC POWER STATION UNDER CONSTRUCTION,
SHOWING SOIL BACKFILLING BEING PLACED AGAINST WALL OF STRUCTURE.

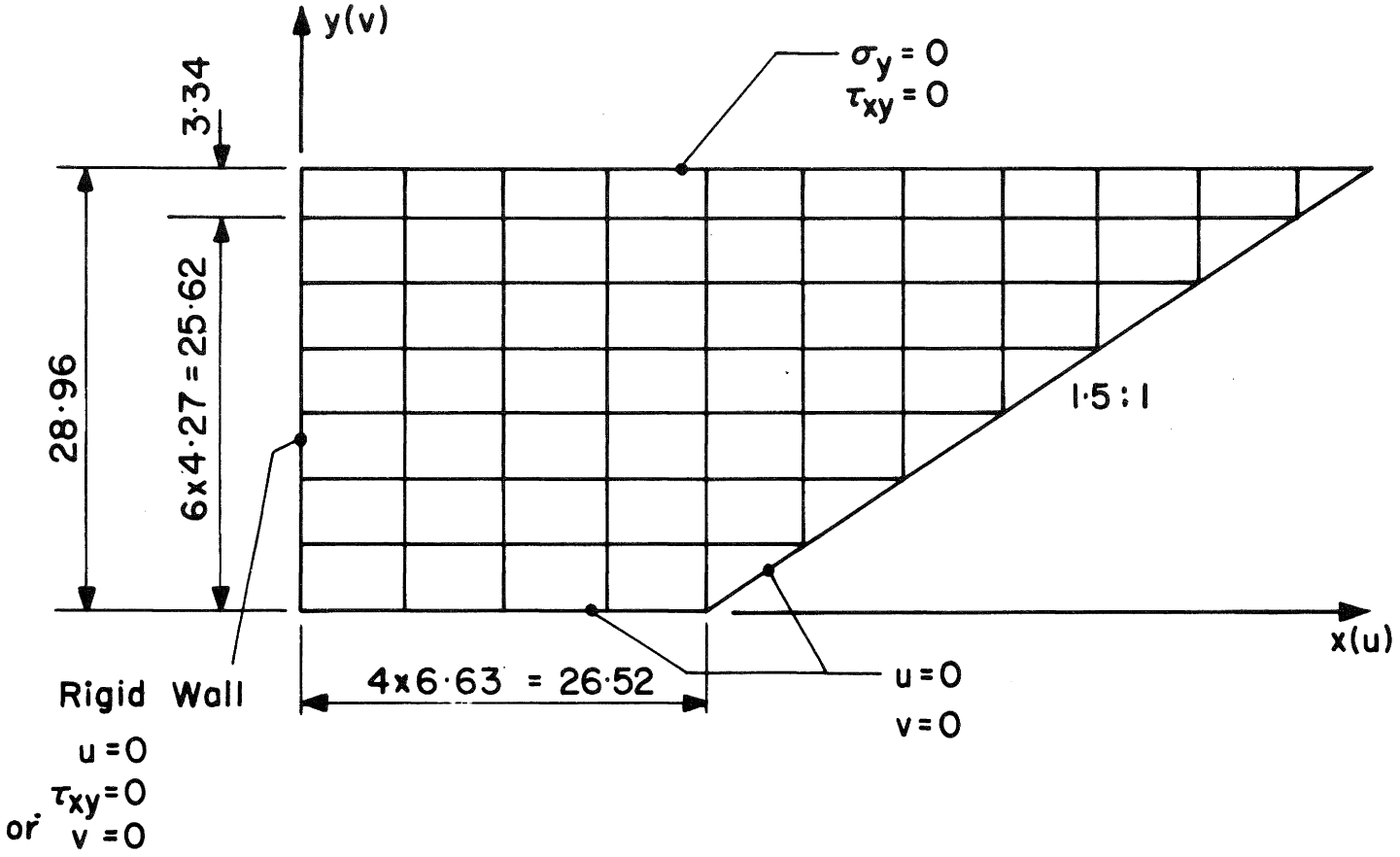

FIGURE 3: FINITE ELEMENT MESH FOR DYNAMIC ANALYSIS.

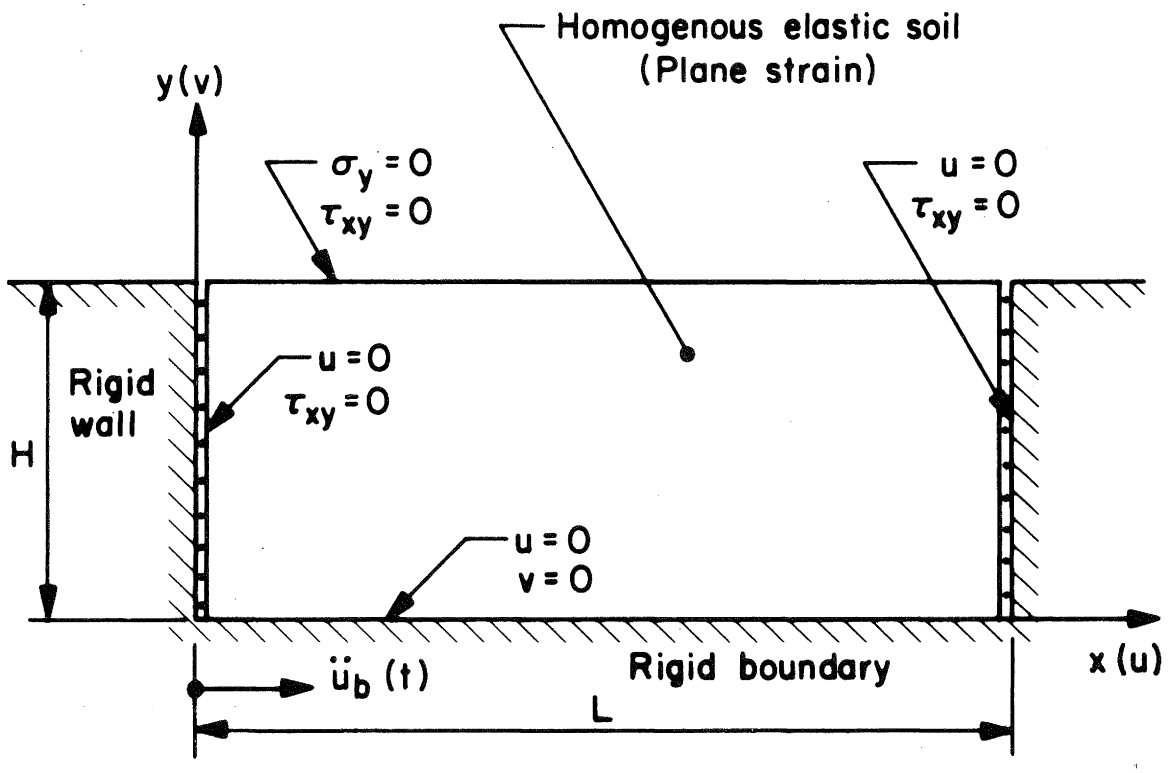

FIGURE 4: RIGID WALL PROBLEM.

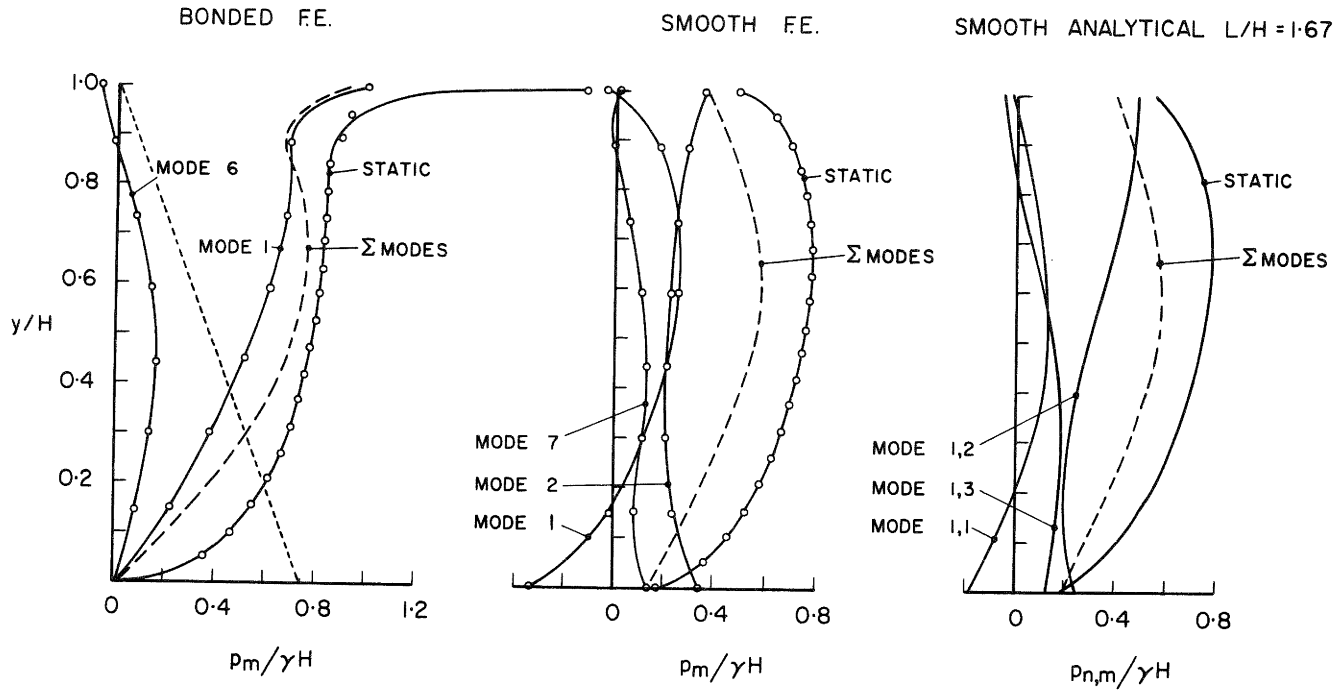

FIGURE 5: STATIC-ONE-G MODAL PRESSURE DISTRIBUTIONS.

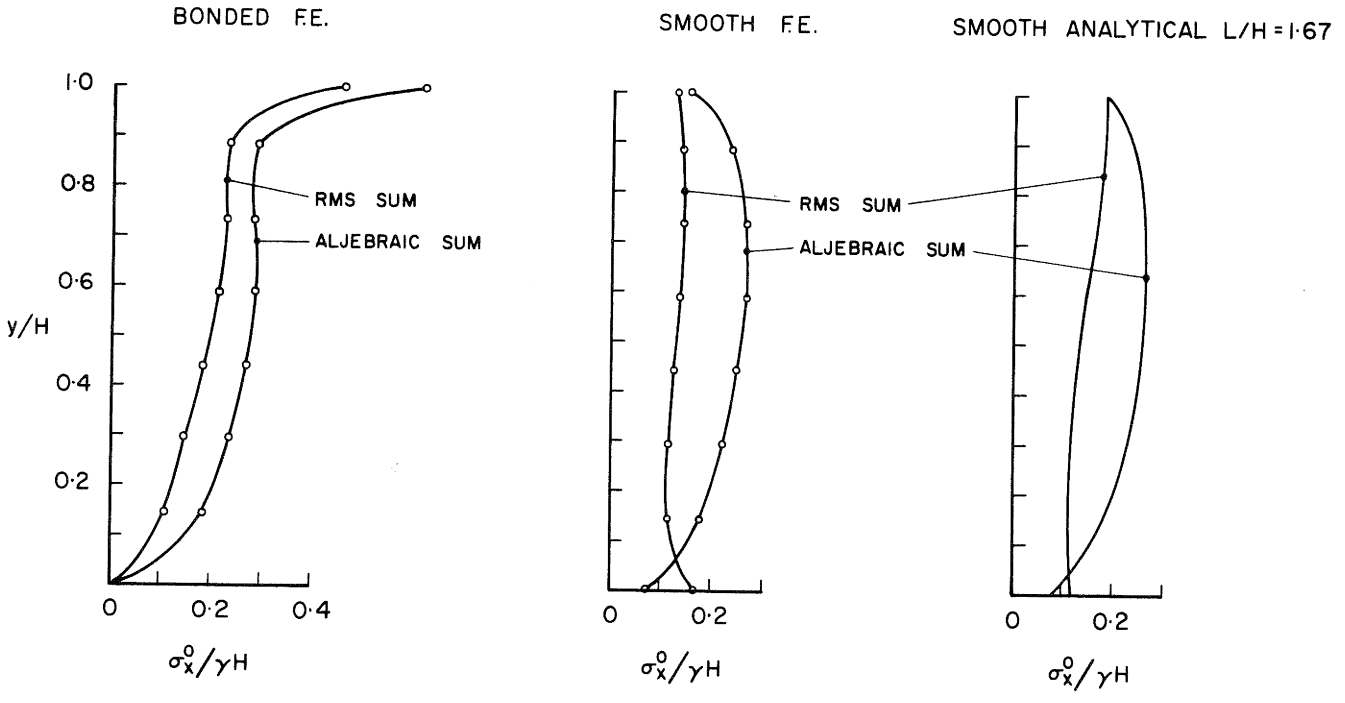

FIGURE 6: MAXIMUM EARTHQUAKE-INDUCED PRESSURES ESTIMATED BY RESPONSE SPECTRUM METHOD.

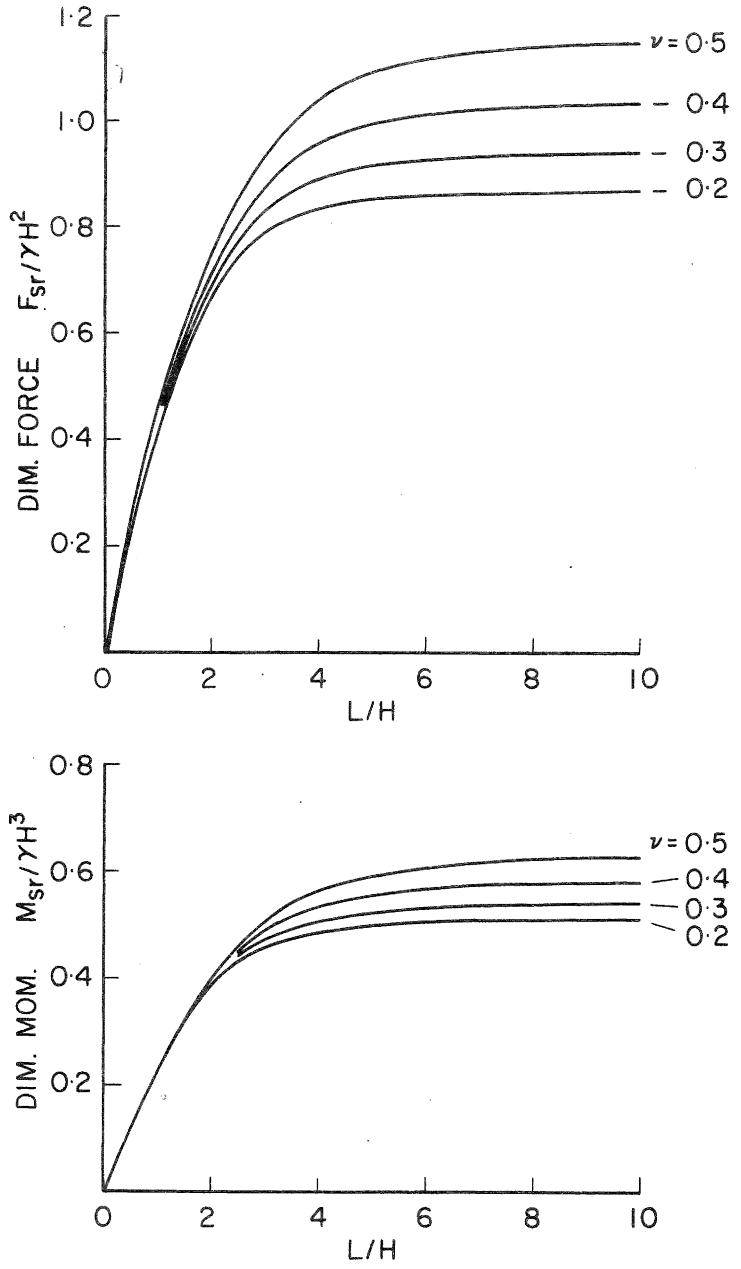

FIGURE 7: FORCE AND MOMENT ON SMOOTH RIGID WALL PRODUCED BY A ONE-G STATIC HORIZONTAL BODY FORCE. ELASTIC SOIL LAYER, LENGTH=L, HEIGHT=H.

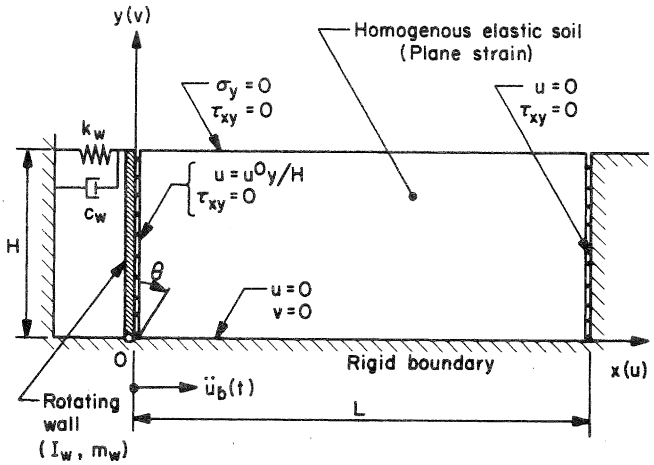

FIGURE 8: ROTATING WALL PROBLEM.

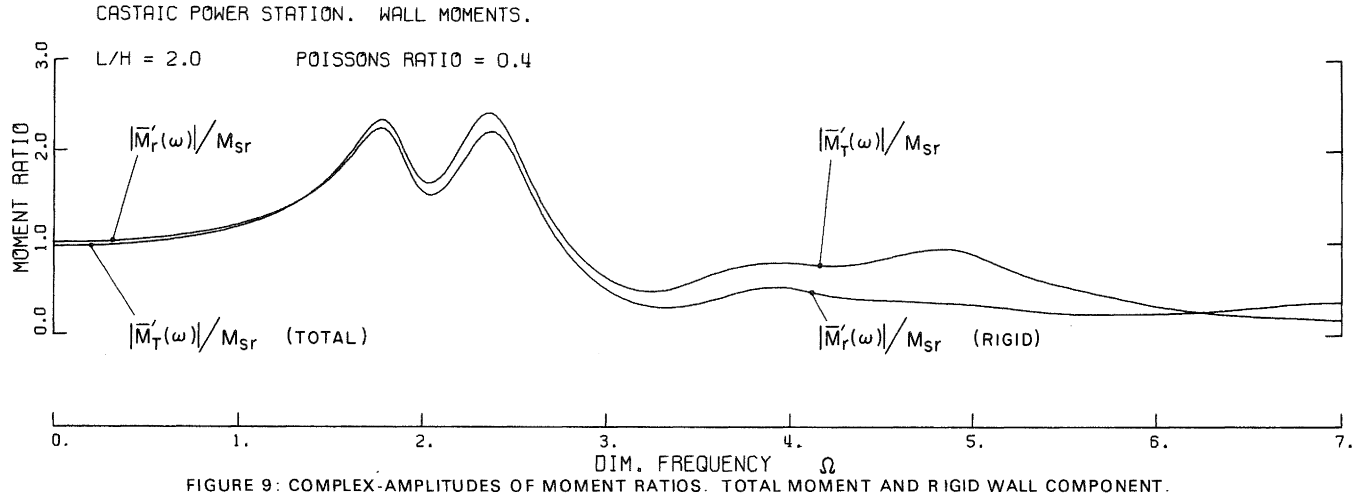

FIGURE 9: COMPLEX-AMPLITUDES OF MOMENT RATIOS. TOTAL MOMENT AND RIGID WALL COMPONENT.

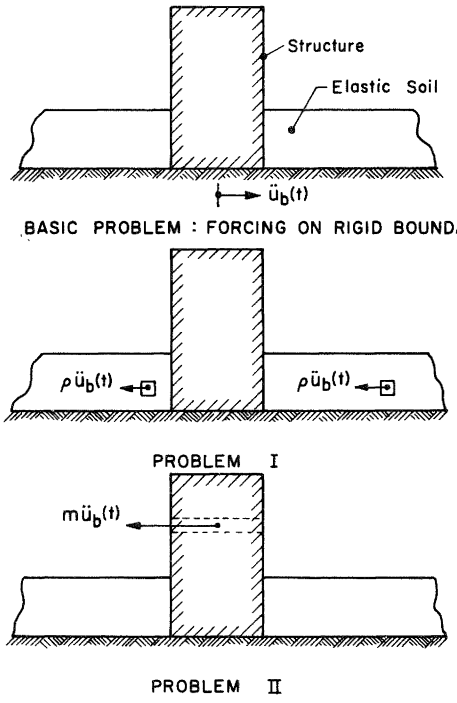

FIGURE 10: APPROXIMATE DYNAMIC ANALYSIS.

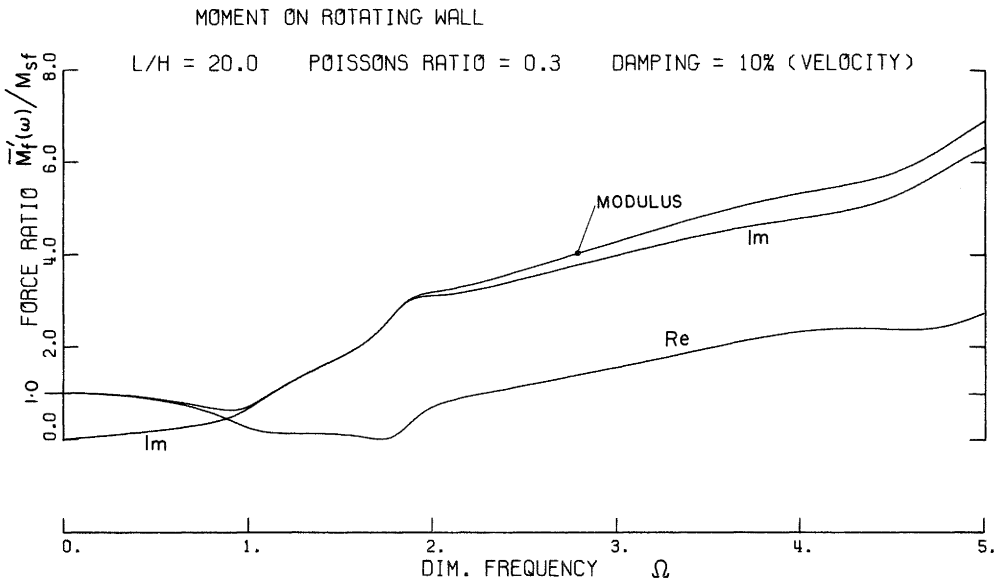

FIGURE 11: COMPLEX-AMPLITUDES OF MOMENT RATIO ON HARMONIALLY FORCED SMOOTH ROTATING WALL. $\frac{L}{H}=20$, $\nu=0.3$.